The solution of the wave equation by wavelets basis approximation

Pascal Joly * Dimitri Komatitsch † Jean-Pierre Vilotte ‡

Enumath conference, September 18-22, 1995, Paris, France

Abstract

This paper is the first development of a work concerning the use of wavelets basis in the numerical solution of the one-dimensional wave equation, that we consider as a good introduction to more realistic two or three-dimensional seismological problems, as it is important to check the accuracy of the tools required for intensive numerical simulation.

The first section of this paper is devoted to the theoretical background : the multiresolution analysis ; in the second section we introduce some associated numerical algorithms and in the last section, we present some numerical results.

AMS(MOS) subject classifications. 65F10

1 Multiresolution Analysis

1.1 Introduction

The multiresolution analysis frame for variational spaces such as $L^2(\mathrm{R})$, has been recently developed by I. Daubechies [6], S. Mallat [14] [15] and Y. Meyer [17] [18].

A multiresolution analysis of $L^2(\mathrm{R})$ is, by definition, an increasing sequence $\{V_j\}_{j\in\mathrm{Z}}$ of closed subspaces having the following properties:

(1) $V_j \subset V_{j+1}$
(2) $f \in V_j \Leftrightarrow f^1 \in V_{j+1}$
(3) $\bigcap_{j\in\mathrm{Z}} V_j = \{0\}$
(4) $\bigcup_{j\in\mathrm{Z}} V_j$ is dense in $L^2(\mathrm{R})$
(5) there exists a function g in V_0, such that $\{g_k\}_{k\in\mathrm{Z}}$ is a Riesz basis of V_0

*C.N.R.S. Laboratoire d'Analyse Numérique. Université Pierre et Marie Curie. Paris
†Laboratoire de Sismologie. Institut de Physique du Globe. Paris
‡Laboratoire de Sismologie. Institut de Physique du Globe. Paris

where by definition

$$\forall f \in L^2(\mathrm{R}),\ \forall x \in \mathrm{R} f^k(x) = 2^{k/2} f(2^k x)$$
$$\forall g \in L^2(\mathrm{R}),\ \forall x \in \mathrm{R}\ \ g_k(x) = g(x-k)$$

1.2 The scaling function

Let us denote φ the function defined by

$$\hat{\varphi}(\omega) = (\sum_{l \in \mathrm{Z}} |\hat{g}(\omega + 2l\pi)|^2)^{-1/2} \hat{g}(\omega)$$

this function satisfies (see [5])

$$\sum_{l \in \mathrm{Z}} |\hat{\varphi}(\omega + 2l\pi)|^2 = 1$$

hence

$$\forall k \in \mathrm{Z} \qquad \int \varphi(x) \times \overline{\varphi(x-k)}\, dx = \delta_{0,k}$$

and then $\{\varphi_k\}_{k \in \mathrm{Z}}$ is an orthonormal basis of the subspace V_0. φ is the so-called scaling function, and it is used to define the subspaces V_j : first define the functions φ_k^j by

$$\forall x \in \mathrm{R},\ \forall j,k \in \mathrm{Z} \qquad \varphi_k^j(x) = 2^{j/2}\ \varphi(2^j\ x - k)$$

For some fixed $j \in \mathrm{Z}$, each orthonormal family $\{\varphi_k^j\}_{k \in \mathrm{Z}}$ generates a subspace V_j, and the sequence $\{V_j\}_{j\ \in \mathrm{Z}}$ is a multiresolution analysis of $L^2(\mathrm{R})$.

1.3 The wavelet function

Now for all $j \in \mathrm{Z}$, let W_j be the orthogonal complementary of V_j in V_{j+1} : $V_{j+1} = V_j \oplus W_j$, then again there exists a function ψ such that $\{\psi_k\}_{k \in \mathrm{Z}}$ is an orthonormal basis of W_0. Furthermore, let us define the functions ψ_k^j by

$$\forall x \in \mathrm{R},\ \forall j,k \in \mathrm{Z} \qquad \psi_k^j(x) = 2^{j/2}\ \psi(2^j\ x - k)$$

each family $\{\psi_k^j\}_{k \in \mathrm{Z}}$ is an orthonormal basis of W_j, and ψ is the so-called wavelet function.

1.4 The bounded domain case

The multiresolution analysis is available in the case of a bounded domain (see for instance [19] and [2]). We are interested in the periodic case on an interval. In [17], Y. Meyer has introduced the periodic multiresolution analysis:

$$\forall\ x \in [0,1] \quad j \geq 0, \quad 0 \leq k < 2^j \qquad \varphi_k^j(x) = 2^{j/2} \sum_{z \in \mathrm{Z}} \varphi(2^j(x+z-k)) \quad .$$

$$\forall\ x \in [0,1] \quad j \geq 0, \quad 0 \leq k < 2^j \qquad \psi_k^j(x) = 2^{j/2} \sum_{z \in \mathrm{Z}} \psi(2^j(x+z-k)) \quad .$$

The functions φ_k^j and ψ_k^j generate subspaces V_j et W_j and define a multiresolution analysis of $L^2(T)$, where T is the torus R/Z, and $L^2(T)$ is a set of 1-periodical functions. We shall use this particular approach in the following; see also [20] for a practical use of these wavelets. Note that the dimension of the subspace V_j is 2^j, so the multiresolution analysis defines a Galerkin approximation of $L^2(T)$.

For numerical experiments, we consider a fixed integer p, the dimension of the corresponding subspace V_p is 2^p, the associated multiresolution is

$$V_p = V_0 \oplus W_0 \oplus W_1 \ldots \oplus W_{p-1}$$

1.5 Some examples of wavelet functions

It is not the aim of this paper to list all available wavelet functions, we just recall some famous ones : the Haar's wavelet function [9] is certainly the oldest example ; there exist also the fast decreasing Meyer's wavelet [17], the compact supported Daubechies' wavelets [6] and the Battle-Lemarié's wavelets with exponential decrease [3], [11].

In the case of G. Battle and P.G. Lemarié's wavelets, both functions φ and ψ are defined by their Fourier transform (see also [7])

$$\hat{\varphi}(\omega) = \frac{1}{(\pi\omega)^m} \frac{sin^m(\pi\omega)}{[P_{m-1}(sin^2(\pi\omega))]^{1/2}}$$

$$\hat{\psi}(\omega) = \frac{e^{-i\omega\pi}}{(\pi\omega/2)^m} \Big[\frac{P_{m-1}(cos^2(\pi\omega/2))}{P_{m-1}(sin^2(\pi\omega/2)) P_{m-1}(sin^2(\pi\omega))} \Big]^{1/2} sin^{2m}(\pi\omega/2)$$

with

$$P_{m-1} \quad (sin^2(z)) = (sin(z))^{2m} \sum_{l \in \mathrm{Z}} \Big(\frac{1}{(z + l\ \pi)} \Big)^{2m}$$

Figure 1 presents the function ψ_0^0, which is used to define all the wavelets functions (level $p = 9$). It is the only basis function of subspace W_0. Figures 2 and 3 show the two basis functions of W_1: ψ_0^1 and ψ_1^1 (note that the real magnitude of the signal is modified).

It is easy to see from figures 4 to 7, that the support length of the basis functions of W_j decreases as j increases. One should also note that the 2^j basis functions of W_j are obtained from ψ_0^j by x-translations of length $k \times 2^{-j}$ (Figures 7 and 8).

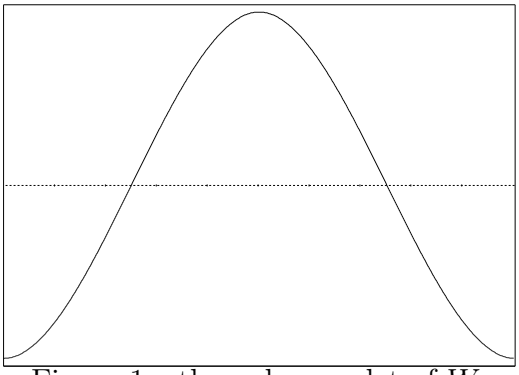

Figure 1 : the only wavelet of W_0

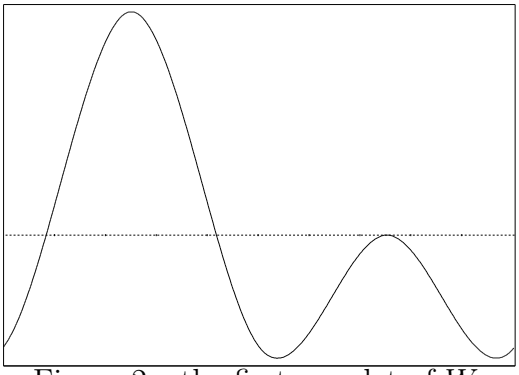

Figure 2 : the first wavelet of W_1

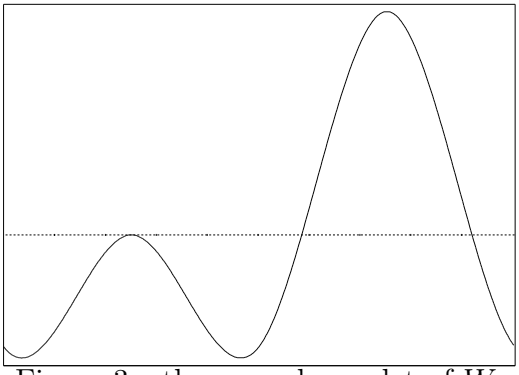

Figure 3 : the second wavelet of W_1

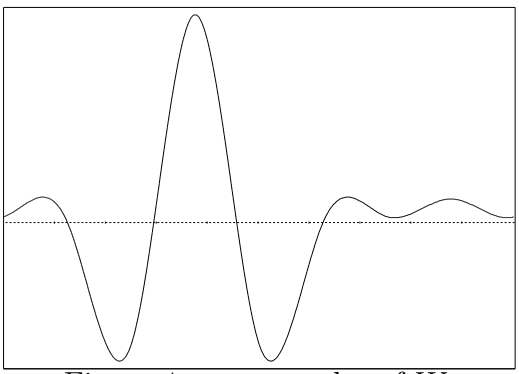

Figure 4 : one wavelet of W_2

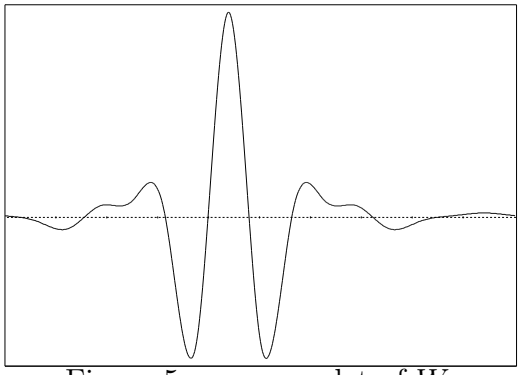

Figure 5 : one wavelet of W_3

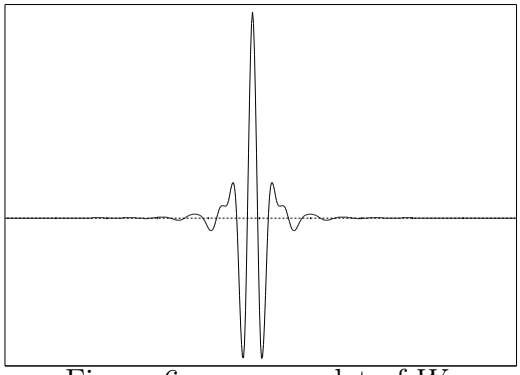

Figure 6 : one wavelet of W_5

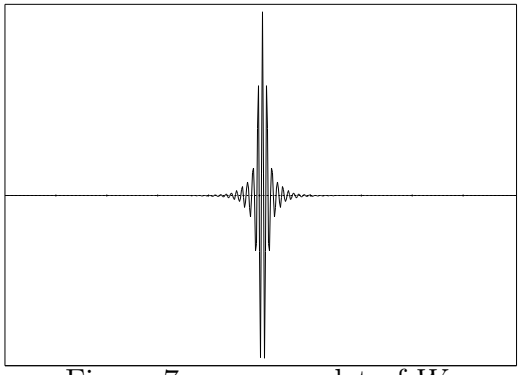

Figure 7 : one wavelet of W_6

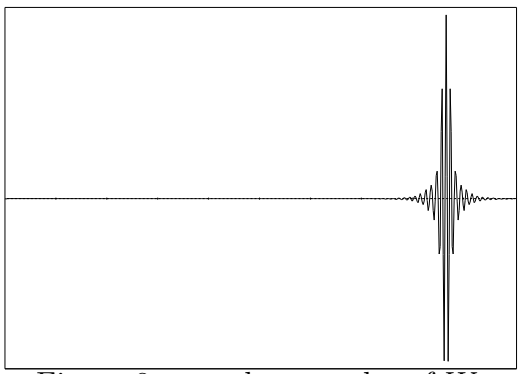

Figure 8 : another wavelet of W_6

2 Algorithms

2.1 Introduction

We present in this section some algorithms that are useful for the different steps of the calculations. The most important step is the determination of the wavelet coefficients, that is the components of some given function $f \in L^2$ in the subspaces W_j, with $0 \leq j < p$, for a multiresolution with p levels. Although the following procedure is available in the general case, we give the formulas in the case of periodic boundary conditions on the interval $[0, 1]$.

The very first step is a to get a regular sampling of the function f, that is the 2^p values $f_k = f(k/2^p)$ $(0 \leq k < 2^p)$; then an interpolation step has to be performed, i.e. find one element $\tilde{f}_p \in V_p \subset L^2$ such that

$$\forall k,\ 0 \leq k < 2^p \qquad\qquad \tilde{f}_p(k/2^p) = f(k/2^p)$$

2.2 Interpolation

We look for the 2^p coefficients c_k^p such that $\tilde{f}_p = \sum_{k=0}^{2^p-1} c_k^p\ \varphi_k^p$.

In the case of the Battle-Lemarié's wavelet, there exists a function $S \in V_p$ satisfying

$$\forall k,\ 0 \leq k < 2^p \qquad\qquad \tilde{S}(k/2^p) = \delta_{0,k}$$

so that the coefficients are defined by (see [20])

$$\forall k,\ 0 \leq k < 2^p \qquad\qquad c_k^p = \sum_{l=0}^{2^p-1} f_l\ L_p(k-l)$$

where

$$\forall k,\ 0 \leq k < 2^p \qquad\qquad L_p(k) = \int_0^1 S(x)\varphi_k^p(x)\ dx$$

2.3 Decomposition

Now we get the 2^p coefficients c_k^p defining an element $f_p \in V_p$; the next step is to obtain the similar coefficients c_k^j in each subspace V_j $(0 \leq j < p)$. This is the decomposition step, for which we use the Mallat transform (see [14]). From the relation

$$V_j = V_{j-1} \oplus W_{j-1}$$

we deduce for any j $(0 < j < p)$

$$\tilde{f}_j = \tilde{f}_{j-1} + \tilde{g}_{j-1} \text{ with } \{ \begin{array}{l} \tilde{f}_{j-1} \in V_{j-1} \\ \tilde{g}_{j-1} \in W_{j-1} \end{array}$$

The 2^j coefficients c_k^{j-1} and d_k^{j-1} satisfy

$$\tilde{f}_{j-1} = \sum_{k=0}^{2^{j-1}-1} c_k^{j-1}\ \varphi_k^{j-1} \qquad \text{and} \qquad \tilde{g}_{j-1} = \sum_{k=0}^{2^{j-1}-1} d_k^{j-1}\ \psi_k^{j-1}$$

the d_k^{j-1} are the so-called wavelet coefficients of level $j-1$.

If we define two discrete 2^j-periodic filters $(G_j(n))_{n\in\mathrm{Z}}$ and $(H_j(n))_{n\in\mathrm{Z}}$ by

$$0 \le j < 2^p \quad G_j(k) = \int_0^1 \varphi_k^j(x)\ \psi_0^{j-1}(x)dx \quad \text{and} \quad H_j(k) = \int_0^1 \varphi_k^j(x)\ \varphi_0^{j-1}(x)dx$$

then (see [20])

$$0 \le k < 2^{j-1} \qquad c_k^{j-1} = \sum_{l=0}^{2^j-1} c_l^j\ H_j(l-2k) \quad \text{and} \quad d_k^{j-1} = \sum_{l=0}^{2^j-1} c_l^j\ G_j(l-2k)$$

To summarize, the decomposition of any function f onto the wavelets basis can be obtained as follows :

- interpolate f on 2^p points with the filter $(L_p(n))_{n\in\mathrm{Z}}$; this leads to an element $\tilde{f}_p \in V_p$.
- proceed p decomposition steps, that is compute the coefficients c_k^{j-1} and d_k^{j-1} from the 2^j coefficients c_k^j $(0 \le k < 2^j)$.

At the end of the pth step, we have computed

- $2^p - 1$ wavelet coefficients d_k^j for $0 \le j < p$ and $0 \le k < 2^j$,
- the mean value $c_0^0 = \int_0^1 \tilde{f}_p(x)\ dx$.

It is important to point out that the decomposition step is reversible, so it is possible to retrieve the 2^p values of $\tilde{f}_p$ from c_0^0 and the $2^p - 1$ wavelet coefficients.

2.4 Computational cost

Most of the computations of the Mallat transform make use of convolution products, that are performed via the Fourier transform, as detailed in the following formulas corresponding to the decomposition step

$$
\begin{array}{c}
(c_n^j) \\
0 \le n < 2^j \\
\downarrow \\
FFT(2^j) \\
\downarrow \\
(\hat{c}^j(k)) \\
0 \le k < 2^j \\
\downarrow \\
\overbrace{\qquad\qquad\qquad\qquad\qquad\qquad}
\end{array}
$$

$$
\begin{array}{cc}
2^j\ \hat{c}^j(k)\overline{\hat{H}}_j(k) & 2^j\ \hat{c}^j(k)\overline{\hat{G}}_j(k) \\
\downarrow & \downarrow \\
FFT^{-1}(2^j) & FFT^{-1}(2^j) \\
\downarrow & \downarrow \\
a(m) & b(m) \\
0 \le m < 2^j & 0 \le m < 2^j \\
\downarrow & \downarrow \\
c_n^{j-1} = a(2n) & d_n^{j-1} = b(2n) \\
0 \le n < 2^{j-1} & 0 \le n < 2^{j-1}
\end{array}
$$

The computational cost of the jth step is then equal to 3 FFT of length 2^j, that is $O(j\ 2^j)$ operations. The total cost of the wavelet decomposition, for a fixed level p, is then

$$3 \times (1 + 2 \cdot 2^2 + \ldots + j \cdot 2^j + \ldots + p \cdot 2^p)$$

that is $O(p\ 2^p)$ operations. The recomposing algorithm proceeds in the reverse order, with the same cost.

2.5 Signal visualization

We present on figure 9 a space-frequency diagram, which is a good way to understand how the decomposition works. To each basis function ψ_n^i is associated a rectangle that represents its support : the horizontal axis stands for the x-dimension, and the vertical axis for the spatial frequencies. Then each horizontal set of rectangles corresponds to a whole subspace W_j : the 2^j rectangles of the set have the same length 2^{-j} and the same height 2^j. This is because subspace W_j samples a specific frequency range $[2^j - 2^{j-1}, 2^j + 2^{j-1}]$, and also because each basis function has a support of length 2^{-j} in the space dimension.

The upper part of figure 9 shows a realistic seismic signal, with the corresponding space-frequency diagram on the lower part. As each rectangle corresponds to a basis function, it is colored in grey if the corresponding component of the signal is greater in magnitude than a threshold parameter (here $\varepsilon = 5 \times 10^{-4}$) ; otherwise it remains white.

For this 9-level multiresolution analysis, only 129 of the 512 components [1] are showed in grey. Note also that this space-frequency representation allows us to show which basis functions are lighted by the signal, so we get an accurate location in space dimension, and also some information on the frequencies contained in the signal. This is one of the most attractive properties of the multiresolution analysis ; unfortunately because all of the rectangles have the same area, it is not possible to have a more accurate location in both space and frequency dimensions.

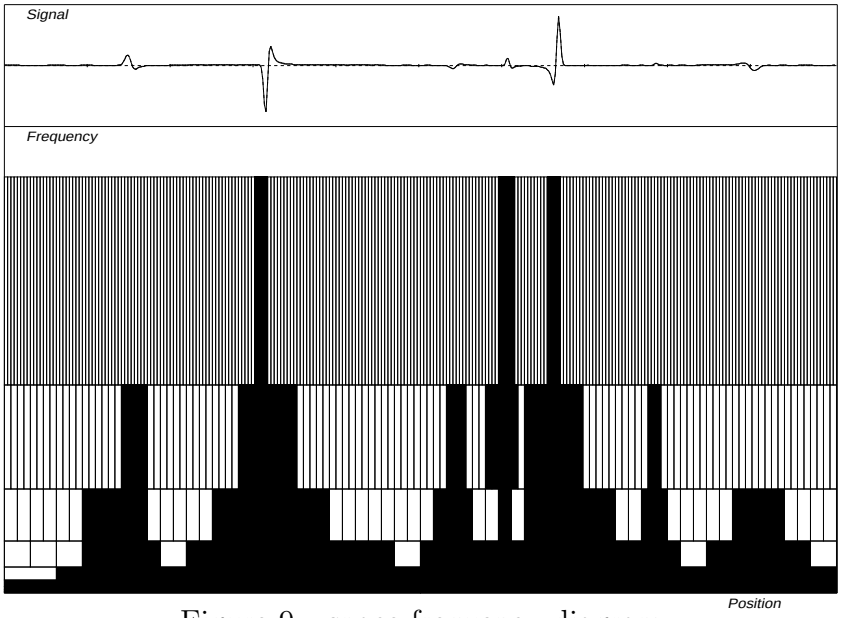

Figure 9 : space-frequency diagram

3 Numerical simulation

3.1 Introduction

The wavelet approximation has been extensively used in signal theory and image processing. More recently the multiresolution frame has been used to solve partial differential equations : see for example J. Liandrat [12], V. Perrier & C. Basdevant [20], R. Glowinski [8], K. Amaratunga & J.R. Williams [1] [24], Y. Maday [13] and P. Joly [10].

In order to solve wave propagation problems that appear in seismology, classical numerical methods are widely used, for instance finite difference methods (Virieux [23]),

[1] it is important to mention that we obtain the same number 129 for a multiresolution of level 11 with 2048 components

spectral or pseudospectral methods (Tessmer [22], Carcione [4]), finite element methods (Marfurt [16]) or spectral element methods (Priolo, Carcione & Seriani [21]). The key point here is to accurately model the propagation of elastic waves and the boundary conditions that, in realistic problems, may essentially be of two different kinds : a rigid boundary condition, i.e. imposing a null displacement on the boundary (Dirichlet), or a free surface condition, i.e. imposing a null traction on the boundary (Neumann conditions or traction-free condition). The free surface condition is, by far, the most widely used in seismology, due to the fact that the Earth's surface itself is a free surface (assuming that the atmosphere layer has approximately the same properties as vacuum).

Note that, in these classical methods, an important number of points have to be used to correctly sample the different wavefronts, and hence the computational cost in 2D and mostly in 3D may be a limitation to the application of these modelling methods to realistic seismological problems. The interest of using a wavelet basis in the modelling scheme clearly appears here : as some of the wavelets of the basis have a thin support in space, we hope that the coefficients associated with these wavelets will be the most significant, and that we will be able to ignore the contribution of the others without significantly degrading the information contained in the signal. Hence this selection process may allow us to represent the signal with a small number of coefficients even in 2D or 3D, and to reduce very significantly the computational cost. Eventhough 1D is not a case for which the most significant improvement is expected, it allows to validate the method.

3.2 The test problem

In this paper, we are interested in the solution of the one-dimensional heterogeneous wave-equation:

$$\rho(x)\ \frac{\partial^2 u}{\partial t^2} - \frac{\partial}{\partial x}(\lambda(x)\ \frac{\partial u}{\partial x}) = 0$$

Parameter λ , also called the Lamé coefficient, is related to the density of the medium ρ and to the velocity of the compression wave in this medium c_p by

$$\lambda = \rho\ c_p^2$$

As the wavelet method is based on the $[0, 1]$ interval with periodic boundary conditions, i.e.

$$\forall t \in [0, T] \qquad\qquad u(0, t) = u(1, t)$$

we use the following transforms for the lengths and the velocities in order to map the physical domain $[0, x_{\max}]$ onto $[0, 1]$, as the equation is linear with respect to these parameters

$$x^{'} = \frac{x}{L}$$

and

$$c_p^{'} = \frac{c_p}{L}\ ,$$

where L is the total length of the elastic bar. The initial conditions are set by prescribing the values of the displacement at the first two time steps, i.e.

$$\forall x \in [0,1] \qquad u(x,0) = u_0(x) \quad , \quad u(x,\Delta t) = u_1(x)$$

where Δt is the time step of the scheme. The solution obtained by the wavelet algorithm is validated by comparing it to an analytical solution in the case of an homogeneous medium and to a finite difference solution in the case of an heterogeneous medium.

3.3 Solution algorithm

We use an explicit second order finite difference scheme for the time extrapolation :

$$u(x,t+\Delta t) = 2\,u(x,t) - u(x,t-\Delta t) + \Delta t^2\,.\,w(x,t)$$

where

$$w(x,t) = \frac{1}{\rho(x)}\,\frac{\partial}{\partial x}(\lambda(x)\,\frac{\partial u}{\partial x}(x,t))$$

and the evolution scheme proceeds with the following steps : suppose that $u(x,t)$ and $u(x,t-\Delta t)$ are known, then $u(x,t+\Delta t)$ can be computed by (u is the real signal, while $\tilde{u}$ stands for its transcription onto the wavelet basis)

$$\begin{array}{ccc}
u(x,t) & \longrightarrow & \tilde{u}(\xi,t) \\
 & & \downarrow \\
\dfrac{\partial u}{\partial x}(x,t) & \longleftarrow & D \times \tilde{u}(\xi,t) \\
\downarrow & & \\
\omega(x,t) = \lambda(x) \times \dfrac{\partial u}{\partial x}(x,t) & \longrightarrow & \tilde{\omega}(\xi,t) \\
 & & \downarrow \\
\dfrac{\partial \omega}{\partial x}(x,t) & \longleftarrow & D \times \tilde{w}(\xi,t) \\
\downarrow & & \\
w(x,t) = \dfrac{1}{\rho(x)}\,\dfrac{\partial \omega}{\partial x}(x,t) & \longrightarrow & \tilde{w}(\xi,t) \\
 & & \downarrow \\
 & & \tilde{u}(\xi,t+\Delta t) = 2\,\tilde{u}(\xi,t) - \tilde{u}(\xi,t-\Delta t) \\
u(x,t+\Delta t) & \longleftarrow & +\Delta t^2\,.\,\tilde{w}(\xi,t)
\end{array}$$

where u is the real signal while $\tilde{u}$ stands for its transcription onto the wavelet basis. Two direct and two inverse Mallat transform, and two matrix by vector products are performed at each time step.

3.4 The derivation matrix

The derivation matrix D is computed in the φ_k^p basis of the subspace V_p:

$$[\mathcal{D}]_{ij} = \int_0^1 \frac{\partial \varphi_i^p}{\partial x}(x)\ \varphi_j^p(x)\ dx = \int_0^1 \frac{\partial \varphi^p}{\partial x}(x - i/2^p)\ \varphi^p(x - j/2^p)\ dx$$

$$= \int_0^1 \frac{\partial \varphi^p}{\partial x}(x - (i-j)/2^p)\ \varphi^p(x)\ dx = d(i-j)$$

with

$$d(i) = \int_0^1 \frac{\partial \varphi^p}{\partial x}(x - i/2^p)\ \varphi^p(x)\ dx \quad \text{and} \quad \varphi^p(x) = 2^{p/2} \sum_{z \in \mathrm{Z}} \varphi(2^p(x+z))$$

The computation of the $(2^p)^2$ coefficients of the initial matrix $\mathcal{D}$ only involves the computation of the 2^p elements $d(k)$; then we perform the Mallat transforms of the 2^p lines of the matrix D, and the transforms of the 2^p columns of the resulting matrix, in order to obtain the expression of matrix D in the ψ_k^j basis.

This part of the simulation is time consuming, but one should note that we can compute and store the derivation matrix once and for all, because it is not related to the particular problem we are dealing with. Hence, it is possible to create a library of derivation matrices (first and second order of derivation) corresponding to different levels of multiresolution, in order to solve any physical problem, set in a partial differential equation form.

3.5 Numerical results

The two test-problems correspond to the initial values

$$u(x,0) = \frac{1}{\sigma^2} \left(\frac{(x - x_c)^2}{\sigma^2} - 1 \right) \exp \frac{-(x - x_c)^2}{2\,\sigma^2}$$

and

$$u(x,\Delta t) = \frac{1}{2\sigma^2} \left(\frac{(x - x_c - c_p \Delta t)^2}{\sigma^2} - 1 \right) \exp \frac{-(x - x_c - c_p \Delta t)^2}{2\,\sigma^2}$$
$$+ \frac{1}{2\sigma^2} \left(\frac{(x - x_c + c_p \Delta t)^2}{\sigma^2} - 1 \right) \exp \frac{-(x - x_c + c_p \Delta t)^2}{2\,\sigma^2} \quad ,$$

with $\sigma = 90$ m and $x_c = 400$ m, c_p being the velocity of the compression wave in the medium. The evolution process requires 1320 time steps Δt of 1.5 ms in order to satisfy a classical Courant-Friedrichs-Levy condition. The multiresolution level is $p = 10$, so the number of unknowns is $2^{10} = 1024$.

The first test-problem corresponds to an homogeneous medium, the density ρ is set equal to 2000 kg.m^{-3} and the velocity c_p is set equal to 1800 m.s^{-1}. Figures 10 and 11 show the computed solution at initial and final instants. Figure 12 shows the analytical solution, together with the residual between the computed and exact solutions drawn at the same scale. An excellent agreement is found. Note that only 51 out of 1024 coefficients are required to represent the initial wave (and 55 for the final one), meaning that the compression rate is high.

The second test-problem corresponds to an heterogeneous medium, the density ρ is set equal to 2500 kg.m^{-3} between 1000 and 2000 m and to 2000 kg.m^{-3} in the remaining part of the domain ; the velocity c_p is respectively equal to 1800 m.s^{-1} and 2200 m.s^{-1}.

Figures 13 and 14 show the computed solution at time steps 600 and 1320 (final instant). Figure 15 shows the solution obtained using a finite difference approximation, together with the residual between the two solutions drawn at the same scale. A good agreement is found between the results given by the two methods.

3.6 Conclusion

The first results of our study of wave propagation problems using wavelets basis approximation are promising, as a good agreement with the analytical and finite difference solutions is found in 1D for two test problems (homogeneous and heterogeneous media). The method may be easily extended to higher dimensions problems without any fundamental modification of the basic approximation scheme.

One of the key points in wave propagation problems in seismology is that most of the energy contained in the signal is located close to the different wavefronts. As in the 1D simulations presented above we get a high compression rate due to the precise spatial localization of some wavelets of the basis, we think that this would be even more significant in 2D or 3D problems where the number of significant coefficients and the computational cost become crucial.

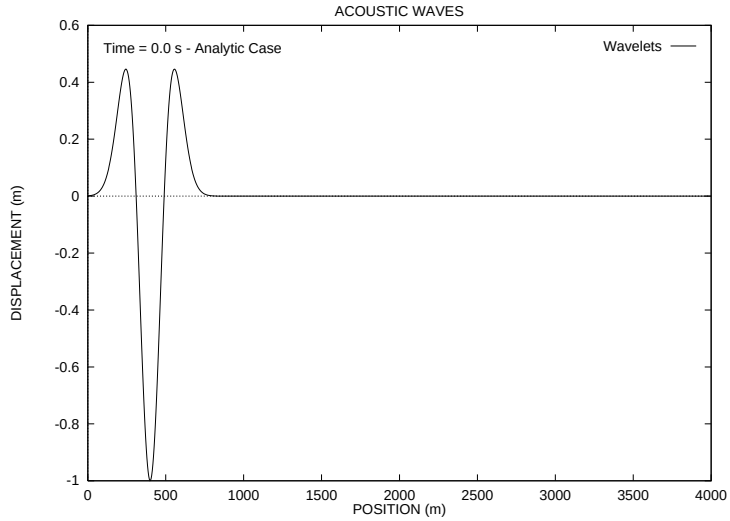

Figure 10 : numerical solution at initial time in the homogeneous case

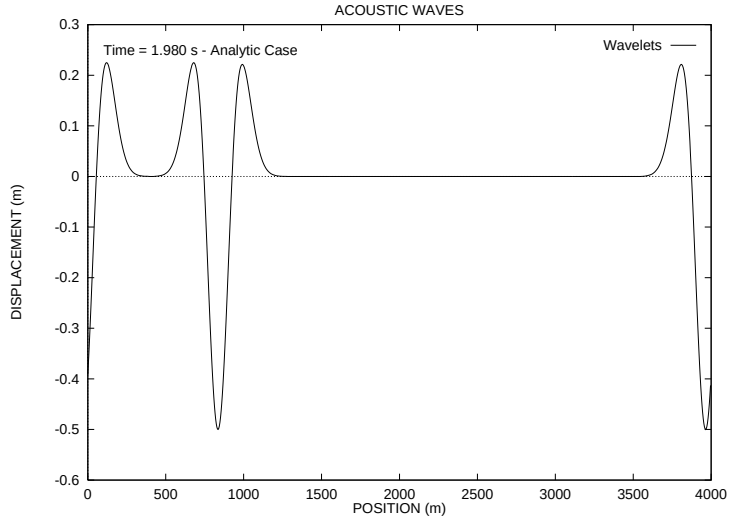

Figure 11 : numerical solution at time $t = 1.98$ s

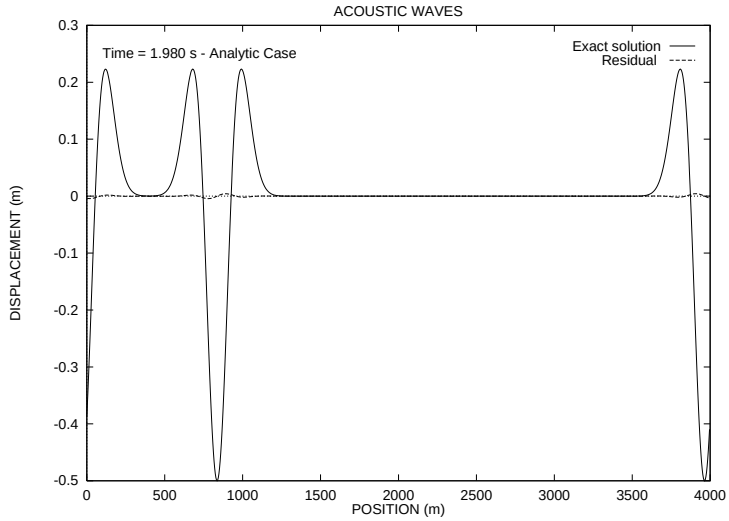

Figure 12 : exact solution and residuals at the same scale at time $t = 1.98$ s

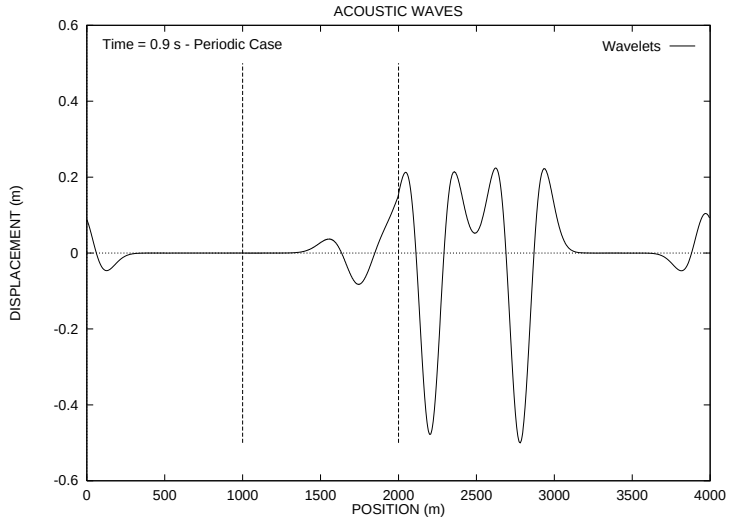

Figure 13 : numerical solution at time $t = 0.9$ s in the heterogeneous case

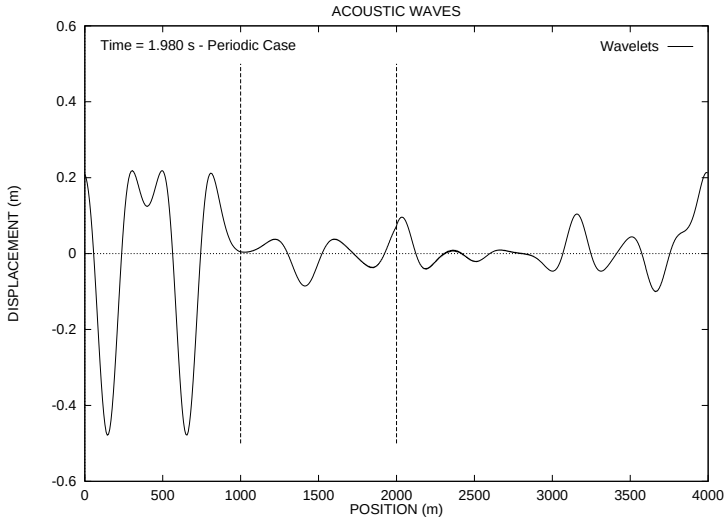

Figure 14 : numerical solution at time $t = 1.98$ s

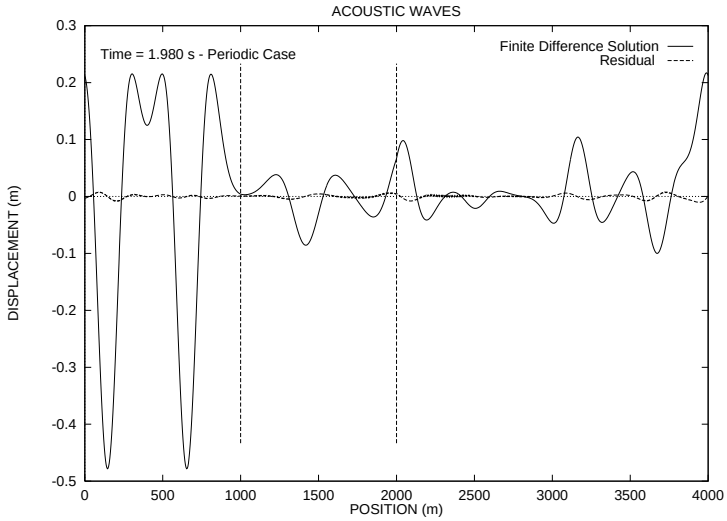

Figure 15 : finite difference solution and residuals at the same scale at time $t = 1.98$ s

References

[1] K. Amaratunga &, J.R. Williams Wavelet-Galerkin solutions for one-dimensional partial differential equations. International Journal for Numerical Methods in Engineering. vol 37 (1994)

[2] P. Auscher Ondelettes à support compact et conditions aux limites. J. Funct. Anal. vol 111 (1993)

[3] G. Battle A block spin construction of ondelettes. Part 1: Lemarié functions. Communications in Mathematical Physics vol 110 (1987)

[4] J.M. Carcione The wave equation in generalized coordinates. Geophysics vol 59 (1994)

[5] A. Cohen Ondelettes et traitement numérique du signal. Masson. Paris (1992)

[6] I. Daubechies Orthonormal bases of supported wavelets. Communications in Pure and Applied Mathematics. vol 41.7 (1988)

[7] C. de Boor A practical guide to splines. Applied Mathematicals Sciences vol 27. Springer (1978)

[8] R. Glowinski, W. Lawton, M. Ravachol & E. Tenebaum Wavelet solution of linear and nonlinear elliptic parabolic and hyperbolic problems in one space dimension. Proceedings of the 9th International Conference on Numerical Methods in Applied Sciences and Engineering. SIAM, Philadelphia (1990)

[9] A. Haar Zur Theorie der orthogonalen Funktionensysteme. Göttingen (1909)

[10] P. Joly Résolution de l'équation de Burgers par paquets d'ondelettes. Publications du Laboratoire d'Analyse Numérique. Université Pierre et Marie Curie. Paris (1995)

[11] P.G. Lemarié Ondelettes à localisation exponentielle. Journal de Mathématiques Pures et Appliquées. vol 67 (1988)

[12] J. Liandrat, V. Perrier & P. Tchamitchian Numerical resolution of Nonlinear Partial Differential Equations using the Wavelet approach. 'Wavelets and their Applications' ed. Ruskai and al. Jones and Barlett (1992)

[13] P. Joly, Y. Maday & V. Perrier Towards a method for solving partial differential equations by using wavelet packet bases. Computer Methods in Applied Mechanics and Engineering. vol 116 (1994)

[14] S.G. Mallat A theory for multiresolution signal decomposition : the wavelet representation. Communications in Pure and Applied Mathematics. vol 41 (1988)

[15] S. Mallat Multiresolution approximation and wavelet orthonormal bases of L^2(R) Transactions of AMS. vol 135 (1989)

[16] K.J. Marfurt Accuracy of finite-difference and finite-element modeling of the scalar wave equation. Geophysics vol 49 (1984)

[17] Y. Meyer Ondelettes, fonctions splines et analyses graduées. Rapport CEREMADE 8703. Université Paris Dauphine (1987)

[18] Y. Meyer Ondelettes et opérateurs. Tomes I à III. Hermann. Paris (1990)

[19] Y. Meyer Ondelettes sur l'intervalle. Rev. Math. Iberoamericana vol 7 (1992)

[20] V. Perrier & C. Basdevant La décomposition en ondelettes périodiques, un outil pour l'analyse de champs inhomogènes. Théorie et algorithmes. La Recherche Aérospatiale. vol 3 (1989)

[21] E. Priolo, J.M. Carcione & G. Seriani Numerical simulation of interface waves by high-order spectral modeling techniques. Journal of the Acoustical Society of America vol 95.2 (1994)

[22] E. Tessmer 3-D seismic modelling of general material anisotropy in the presence of the free surface by a Chebyshev spectral method. Geophysical Journal International vol 121 (1995)

[23] J. Virieux P-SV wave propagation in heterogeneous media : velocity-stress finite-difference method. Geophysics vol 51 (1986)

[24] J.R. Williams, K. Amaratunga Introduction to wavelets in engineering. International Journal for Numerical Methods in Engineering. vol 37 (1994)